

## FATIGUE PROPERTIES OF STEEL AFTER PLASMA NITRIDING PROCESS

STUDENY Zbynek<sup>1,a</sup>, POKORNY Zdenek<sup>1,b</sup>, DOBROCKY David<sup>1,c</sup>

<sup>1</sup> University of Defense in Brno, Department of Mechanical Engineering, Brno, Czech Republic, EU

<sup>a</sup> [zbynek.studeny@unob.cz](mailto:zbynek.studeny@unob.cz), <sup>b</sup> [zdenek.pokorny@unob.cz](mailto:zdenek.pokorny@unob.cz), <sup>c</sup> [david.dobrocky@unob.cz](mailto:david.dobrocky@unob.cz)

### Abstract

The paper deals with the steel 41CrAlMo7-10 fatigue characteristics changes following the plasma nitriding process. Two sets of samples were heat-treated identically. Then they were subjected to a plasma nitriding process. The mixture rate of basic gases, hydrogen and nitrogen, forming the atmosphere during the plasma nitriding, was mutually inverted. Process parameters such as the time, applied voltage and pulse length were identical for both sets. Following the heat treatment and surface coating formation of the diffusion layer of nitrides both sets were subject to *rotating bending fatigue testing* in the machine R.R.Moore L2568 of Instron Co. The fatigue tests were carried out in accordance with the CSN 42 0363 Fatigue Testing of Metals, Methodology of Testing. Then, the tests were evaluated numerically and graphically using Wöhler's (S-N) curve in a semi-logarithmic form. The testing resulted in either the test sample fracture, or at completion  $10^7$  cycles. Evaluated were inclusions in the test bar fractures whereat the stress nucleation and fracture initiation took place. Calculated was the stress intensity factor  $\Delta K_{I_{max}}$  declared in  $\text{MPa}\cdot\text{m}^{0.5}$ . Thanks to the completed testing, derived and analysed results new knowledge was acquired in the field of plasma nitriding steels.

**Keywords:** Plasma nitriding, 41CrAlMo7-10 steel, fatigue

### 1. INTRODUCTION

Plasma nitriding processes are based on the diffusion of atomic nitrogen onto the nitrated steel or cast iron surface like other nitriding variants that depend on the presence of atomic nitrogen on the metal surface. They rank among the most effective nitriding techniques. At elevated temperature the atomic nitrogen is able to penetrate through the surface nitride adsorption layer into the lattice of the parent metal and diffuse further into steel. On the nitrated part surface is formed a compound layer, the so-called white nitride layer, usually consisting of  $\epsilon\text{-Fe}_{2-3}\text{N}$  and  $\gamma\text{-Fe}_4\text{N}$  type iron nitrides. There is a diffusion layer under the compound layer of nitrides. The diffusion layer is formed by dispersed/distributed nitrides of iron and alloying elements having high affinity to nitrogen [1, 2]. The properties and composition of the nitride layers can be influenced by the plasma nitriding process conditions, which are: voltage, time, temperature, composition of the nitriding atmosphere with a ratio of  $\text{H}_2:\text{N}_2$  (usually  $1\text{H}_2:3\text{N}_2$  or reciprocally  $3\text{H}_2:1\text{N}_2$  and finally the surface condition [3]. Plasma nitriding has been so far used on components, above all to increase the surface hardness. Higher surface hardness radically augments the resistance to wear and thereby extends the working lifespan of components. Unexploited in a larger scope of applications are other two useful effects of plasma nitriding, i.e. the increased fatigue strength and improved corrosion resistance of metals. If the fatigue properties are to augment it is undesirable to have the nitrated surface coated by the white layer. Yet this layer is essential for corrosion resisting purposes. It is relatively brittle, for that reason by far breakable. The resultant crack may behave as a stress concentrator and result in an additional failure of the component. This article deals primarily with a less utilized plasma nitriding option, i.e. the increase of fatigue properties in the nitriding steel 41CrAlMo7-10.

### 2. SAMPLE PREPARATION

The experiments involved two series of samples. Each series contained 15pcs of experimental rods. The rods were lathe turned to a diameter of 8 mm. After the heat treatment as per **Table 1** the wastage allowance

exceeding the final shape was ground off. The rod consists of two chucking parts of 7.61 mm in diameter and of 19 mm in length, held tightly via chucking jaws in the bearings. Between the chucking parts is the functional section of 5.2 mm in diameter, which is expected to fracture. The total length of the rod is 87 mm. Ideally, a fracture occurs approximately in the middle of the test rod functional part because of the maximum bending moment. Transition radii of the chucking and functional parts are chosen so as they should not cause stress concentrators. The manufacturing technologies have to be realized so as to avoid undercuts, or prevent surface hardening. Undercuts would act as stress concentrators and could invalidate the test results. Surface hardening might affect the diffusion processes during the following final test bar surface treatment process, i.e. the plasma nitriding. The resultant surface roughness in the chucking portion is  $R_a = 0.8 \mu\text{m}$ . Such roughness was chosen because of reliable chucking of the test bar in the jaws. The resultant surface roughness in the test bar functional part was set to the value of  $R_a = 0.2 \mu\text{m}$ , which is consistent with the standard CSN 42 0363 [4]. The last technological operation, i.e. the sample surface treatment using the plasma nitriding process was conducted in the PN 60/60 from Rübige Co. The method and results of this process are presented in **Table 2**. Voltage (530 V), pressure (280 Pa) and the pulse length (120 ms) were identical for both series. The samples were divided into two sets - A2 and A4. The plasma nitriding parameters differed only in the applied nitriding atmosphere, which was chosen with mutually inverted gas ratios. For A2 set it was used "standard atmosphere" with a gas mixture of  $\text{H}_2$  and  $\text{N}_2$  in the ratio of 1 : 3 and for A4 set was chosen "inverted atmosphere", a gas mixture of  $\text{H}_2$  and  $\text{N}_2$  in the ratio of 3 : 1.

**Table 1** Method for the sample heat-treating process

Operation	Temperature [°C]	Time [min]	Cooling environment
Normalizing	900	25	Air
Quenching	930	25	Oil
Tempering	640	40	Oil

**Table 2** Plasma nitriding process and results

Sample series	Temperature [°C]	Time [h]	Environment ( $\text{H}_2:\text{N}_2$ ) Flow rate [l/h]	White layer depth [ $\mu\text{m}$ ]	Diffusion layer depth [ $\mu\text{m}$ ]
A2	500	20	8:24	$8.7 \pm 1$	<b>344</b>
A4	500	20	24:8	$1.9 \pm 0.3$	<b>304</b>

### 3. PERFORMING EXPERIMENTS

#### 3.1. Fatigue test

There are some particulars in carrying out the rotating bending fatigue testing under laboratory conditions. First is the requirement for geometric accuracy and surface quality in manufacturing the samples. In the case of cylindrical test samples to be used in the rotating bending fatigue test, great attention is to be paid to the alignment of the chucking parts and the functional part responsible for the suppression of sample circumferential run-out. On stepping up the load during the rotation, oscillations will appear and go up even at relatively small peripheral run-out, typically leading to excessive heating of the sample and, as a rule, to automatic cut-off of the test machine in order to secure safety in the test procedure. The standard CSN 42 0363 [4] defines temperature for the test. If exceeded, the test will be annulled and its outcome removed from the subsequent calculating and creating Wöhler's curve. Similar emphasis is laid on the surface quality,

especially on the roughness. Surface roughness requirements for the sample chucking part differ from those for the functional part.

The test specimen rods are either smooth without any notches and/or vice versa with a notch acting as a stress concentrator for the notch coefficient determination. According to Hörger O. [5] the fatigue limit does not depend on the rod length. However, the rod length is influenced by the particular specifications of the test machine design.

The experiment done on Instron R.R. Moore L2568 system was conducted in accordance with the CSN 42 0363 Standard [4]. The load weight of first sample was just under the yield strength (at about 80% Rp 0.2). The load weights of other specimens were gradually varied by ever-lowering tension value to achieve the level of load at which the experimental specimens endured  $10^7$  cycles.

### 3.2. Stress intensity factor

In the vicinity of the fatigue crack tip arise significant quantitative and qualitative changes in the stress and strain field, which can be characterized by one of the fracture mechanics parameters, most often the stress intensity factor  $K$ . The resulting conduct of the crack is caused by the interaction of mechanical stress and the material structure in the process zone ahead of the crack tip, also influenced by temperature and environment [6]. On these fracture-mechanical parameters of fatigue cracks, among other things, also depends the fatigue crack propagation rate  $da / dN$ . Finding that this rate is controlled by range of stress intensity factor  $\Delta K$ , is one of the most important discoveries in the field of material fatigue research. The stress intensity factor  $K$ , like other parameters of fracture mechanics, such as the crack driving factor  $G$ , strain energy density factor  $S$ , crack tip development CTOD,  $J$ -integral, and other, is a complex parameter, quantifying the influence of a wide range of diverse factors. This fact can be expressed by the general Equation [6]:

$$K = K(\sigma, a, L, M) \quad (1)$$

where:

- $\sigma$  - refers to the set of factors characterizing the load of the body;
- $a$  - symbolically indicates the set of parameters describing the number, size, shape, position of cracks within the tested body;
- $L$  - is the set of parameters describing the shape and dimensions of the body, including possible structure indentations such as holes, grooves and recesses;
- $M$  - refers to the parameters relating to the material mechanical properties, which are elastic constants, i.e. tensile modulus and shear strength, Poisson's ratio.

The stress intensity factor value for the given case can be determined e.g. analytically, numerically or experimentally. If we know the value of the stress intensity factor  $K$ , we can determine the quantities characterizing the stress and strain in the nearest vicinity of the crack tip. In the fatigue crack propagation area close to inclusion Murakami [7] worked on the stress intensity factor formula. He arranged the resulting equation into the form:

$$\Delta K_{\text{Imax}} \approx 0,65 \cdot \Delta \sigma \cdot \sqrt{\pi \cdot A_p} \quad (2)$$

$\Delta K_{\text{Imax}}$  value given in  $\text{MPa} \cdot \text{m}^{0.5}$  was derived for an ellipsoidal space inclusion as the maximum stress intensity factor. The quantity  $A_p$  in the equation (2) expresses cross-sectional area inclusion in the plane perpendicular to the direction of the stress in meters and the parameter  $\Delta \sigma$  expresses stress given in MPa. Assuming  $\Delta K$  to be a critical parameter affecting the fatigue crack propagation rate, then the relation between the value of the stress intensity and fatigue life span is quite evident, represented by the number of cycles till the fracture of the component [8].

## 4. RESULTS AND DISCUSSION

### 4.1. Results of fatigue tests

Following the above preparation of the samples they were subjected to *rotating bending fatigue testing* on the *rotating bending fatigue testing* machine R.R.Moore L2568 of Instron Co. Samples were loaded under the same climatic conditions at 20 °C ± 1 °C and relative humidity 60 % ± 5 %. The applied load in the form of disks calibrated in kilograms was then reduced to stress in MPa. The maximum values of voltage were chosen with respect to the yield strength of the tested material. Further lower or higher levels of stress were selected in accordance with the standards CSN 42 0363 [4] and CSN 42 0368 [9] following a minimum step of 15 MPa for the sufficient number of samples to create reliably Wöhler's curve. Two to three samples were tested at each selected voltage level because of accuracy and reliability of the measured results [2].

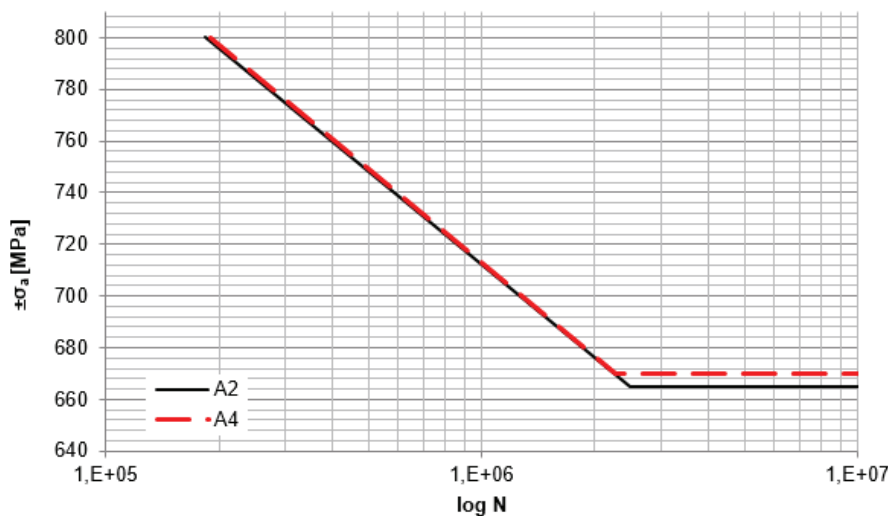


**Figure 1** Wöhler's (SN) curves of A2 and A4 series

**Table 3** shows the resultant values of fatigue strength  $\sigma_c$  MPa for both series of samples. **Table 3** also provides equations of the sloping part of SN curves obtained by linear regression, and the value of reliability  $R^2$ . If the samples exceeded the number of cycles  $10^7$  and no fracture occurred, the experiment was stopped in agreement with the above standard CSN 42 0363 [4].

The resultant values of the fatigue tests were approximated using the equation for straight line,

$$\log \sigma_a = A + B \cdot \log N_f \quad (3)$$

and Wöhler's (SN) curves were obtained by the regression analysis using the equation:

$$\sigma_a = \sigma_f (2N_f)^b \quad (4)$$

The resultant Wöhler's curves are shown in a semi-logarithmic form  $\sigma_a$  - log NSF in **Figure 1**.

There was a slight increase in fatigue strength when changing the parameters of the atmosphere, i.e. inverting the main gas ratios during the plasma nitriding process. Results can be seen in **Table 3**. The increase of fatigue strength  $\sigma_c$  in A4 sample series is the outcome of a significant change in the white layer depth. The white layer for A4 attained the depth of 1.9  $\mu\text{m}$ . Since the white layer is a source of surface cracks during loading for its hardness but brittleness [2], its thinning had positive effect on the fatigue characteristics, particularly on the value of the fatigue strength  $\sigma_c$ .

**Table 3** Fatigue test results

Series	Fatigue strength $\sigma_c$ [MPa]	Regression equation	Reliability value
A2	665	$y = -50.3\ln(x) + 1406$	$R^2 = 0.977$
A4	670	$y = -51.7\ln(x) + 1425$	$R^2 = 0.993$

#### 4.2. Determining the stress intensity factor

The stress intensity factor  $\Delta K$  graphical result calculation according to equation (2) for A2 and A4 plasma nitrided series is obvious from **Figure 2**. The calculation results are shown as two groups of points for each sample series. If aligning the trends, the decreasing dependence of stress intensity factor  $\Delta K$  on the number of cycles to the fracture is apparent. The calculation of points in **Figure 2** includes only the samples for which the fracture occurred at all sets. Equation (2) provides obvious dependence of  $\Delta K$  value on the inclusion cross-section, i.e. its size and stress value  $\sigma_a$  [MPa]. It follows from this dependence that at the increasing number of cycles and decreasing voltage the critical size of inclusion needed to initiate the fracture reduces. It is apparent from the dependence in **Figure 2** that when the high-cycle fatigue phase was approaching the influence of time on the plasma nitriding process decreased. Essential is the difference in the value of the stress intensity factor, and thus also in the cross-sectional size of the inclusion with respect to the load trend in dependence on the standard or inverted atmosphere in the plasma nitriding process.

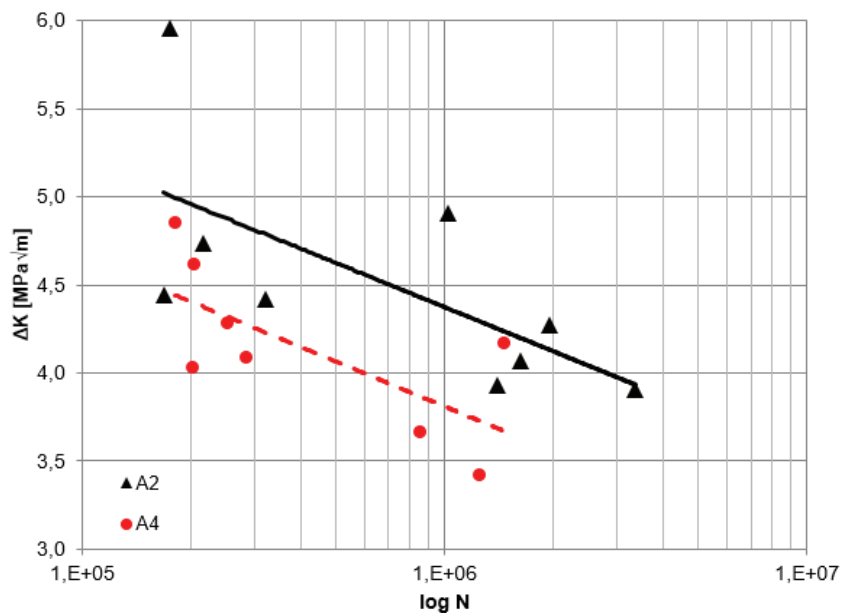


**Figure 2** The stress intensity factor curve

## 5. CONCLUSIONS

The article analyses the fatigue characteristics for steel 41CrAlMo7-10 refined by heat treatment and plasma nitriding process. This steel was used to prepare two sets of samples, which were plasma nitrided in standard atmosphere (Set A2) and in inverted atmosphere (set A4) environments. Main parameters of plasma nitriding and resulting values of the layer following the above process are summarized in **Table 2**. Samples were subjected to *rotating bending fatigue testing* on experimental apparatus R.R.Moore L2568 from Instron Co. Set A2 achieved fatigue strength  $\sigma_c = 665$  MPa. Set A4, with the inverted ratio of gases in plasma nitriding environment, achieved higher fatigue strength  $\sigma_c = 670$  MPa. This increase is due to a significant thinning of the white layer, which is created on the surface of plasma nitrided components however, its hardness and

brittleness may be a source of cracks. Such a change may be considerable especially for the fatigue tests, which are characterized by a high-cycle load.

As seen in **Table 2** the inverted atmosphere in the plasma nitriding process resulted in a radically thinner white layer. With A2 series, using atmosphere  $H_2:N_2 = 1 : 3$ , the white layer depth attained 8.7  $\mu m$ . With A4 series, plasma nitrided in inverted atmosphere  $H_2:N_2 = 3 : 1$ , the depth of white layer was only 1.9  $\mu m$ . This radical thinning of the very hard and brittle compound white layer correlate with lower values of the stress intensity factor  $\Delta K$  with A4 series compared with A2 series, and indicates longer fatigue life span of samples following the plasma nitriding. At the same time, it leads to a reduction in the cost of the process itself thanks to a more suitable choice of gas.

Future prospects are in comparing the results after 20hr of plasma nitriding with shorter or if need be longer processing time. It will also be beneficial to correlate the resulting effects with other types of structural steel of chemical composition suitable for the plasma nitriding treatment.

## ACKNOWLEDGEMENTS

*The paper has been prepared thanks to the support of the project **The Development of Technologies, Design of Firearms, Ammunition, Instrumentation, Engineering of Materials and Military Infrastructure "VÝZBROJ (DZRO K201)" and "Povrchové technologie v aplikacích speciální techniky SV16-216"**.*

## REFERENCES

- [1] HRUBÝ, V., LIPTÁK, P., POKORNÝ, Z. Plasma Nitriding of Cavities, Rzeszów, ISBN 978-83-63666-93-4, (2013)
- [2] STUDENÝ, Z. Analysis of the Influence of Initiating Inclusions on Fatigue Life of Plasma Nitrided Steels. *Manufacturing Technology*, 2015, vol. 15, no. 1, p. 99-105. ISSN 1213-2489.
- [3] POKORNÝ, Z., HRUBÝ, V., STUDENÝ, Z. Effect of nitrogen on surface morphology of layers. *Metallic Materials*, 2016, vol. 54, no. 2, p. 1-6. ISSN 0023-432X.
- [4] ČSN 42 0363 Zkoušky únavy kovů. Metodika zkoušení (Metal Testing. Fatigue Testing of Metals. Methodology of Testing).
- [5] KLESNIL, M., LUKAŠ, P. Únava kovových materiálů při mechanickém namáhání (Fatigue of Metallic Materials under Mechanical Stress). Academia Praha (1975)
- [6] KUNZ, L. Šíření únavových trhlin z hlediska lineární lomové mechaniky (Fatigue Crack Propagation in Terms of Linear Elastic Fracture Mechanics). In: Letná škola únavy materiálů 2006 Summer School of fatigue materials 2006, Žilina - Strečno, p. 19-30, ISBN 80-8070-582-8, SR (2006)
- [7] MURAKAMI, Y. Metal Fatigue, Effect of Small Defects and Non-metallic Inclusions. Elsevier publ., Oxford, UK (2002)
- [8] LAMBRIGHTS, K., at col. Influence of Non-metallic Inclusions on the Fatigue Properties of Heavily Cold Drawn Steel Wires. *Procedia Engineering* 2, p. 173-181 (2010)
- [9] ČSN 42 0368 Zkoušky únavy kovů. Statistické vyhodnocování výsledků zkoušek únavy kovů (Metal testing. Fatigue Testing of Metals. Statistical Evaluation of Fatigue Test Results of Metals).